



# A novel computationally engineered collagenase reduces the force required for tooth extraction in an *ex-situ* porcine jaw model

Tamar Ansbacher<sup>1,2†</sup>, Ran Tohar<sup>1†</sup>, Adi Cohen<sup>1</sup>, Orel Cohen<sup>1</sup>, Shifra Levartovsky<sup>3</sup>, Adi Arieli<sup>3</sup>, Shlomo Matalon<sup>3</sup>, Daniel Z. Bar<sup>1</sup>, Maayan Gal<sup>1\*†</sup> and Evgeny Weinberg<sup>1,4\*\*†</sup>

## Abstract

The currently employed tooth extraction methods in dentistry involve mechanical disruption of the periodontal ligament fibers, leading to inevitable trauma to the bundle bone comprising the socket walls. In our previous work, we have shown that a recombinantly expressed truncated version of clostridial collagenase G (ColG) purified from *Escherichia coli* efficiently reduced the force needed for tooth extraction in an *ex-situ* porcine jaw model, when injected into the periodontal ligament. Considering that enhanced thermostability often leads to higher enzymatic activity and to set the basis for additional rounds of optimization, we used a computational protein design approach to generate an enzyme to be more thermostable while conserving the key catalytic residues. This process generated a novel collagenase (ColG-variant) harboring sixteen mutations compared to ColG, with a nearly 4°C increase in melting temperature. Herein, we explored the potential of ColG-variant to further decrease the physical effort required for tooth delivery using our established *ex-situ* porcine jaw model. An average reduction of 11% was recorded in the force applied to extract roots of mandibular split first and second premolar teeth treated with ColG-variant, relative to those treated with ColG. Our results show for the first time the potential of engineering enzyme properties for dental medicine and further contribute to minimally invasive tooth extraction.

**Keywords** Collagen, Collagenase, Protein engineering, Tooth extraction, Minimally invasive medicine

<sup>†</sup>Tamar Ansbacher and Ran Tohar equal first authors.

<sup>†</sup>Maayan Gal and Evgeny Weinberg contributed equally to this study.

\*Correspondence:

Maayan Gal  
mayyanga@tauex.tau.ac.il  
Evgeny Weinberg  
evgenywein@gmail.com

<sup>1</sup> Department of Oral Biology, Goldschleger School of Dental Medicine, Faculty of Medicine, Tel Aviv University, 6997801 Tel Aviv, Israel

<sup>2</sup> Hadassah Academic College, 91010 Jerusalem, Israel

<sup>3</sup> Department of Oral Rehabilitation, Goldschleger School of Dental Medicine, Faculty of Medicine, Tel Aviv University, 6997801 Tel Aviv, Israel

<sup>4</sup> Department of Periodontology and Oral Implantology, Goldschleger School of Dental Medicine, Faculty of Medicine, Tel Aviv University, 6997801 Tel Aviv, Israel

## Introduction

Exodontia (i.e., tooth extraction) is among the most common clinical procedures in dentistry [1, 2]. The attachment of the tooth to the alveolar bone is primarily carried out with a group of collagen fibers known as periodontal ligament (PDL). Thus, regardless of the tooth extraction method, an important component required for safe tooth removal is careful disruption of the collagen fibers of the PDL, followed by the accurate delivery of the intact tooth [3, 4]. However, given the need for the application of additional surgical procedures such as root separation, reflection of a mucoperiosteal flap and removal of alveolar bone to gain access to the remnants of tooth roots, dental extraction potentially becomes a considerably invasive procedure [5, 6]. Such a procedure often creates



damage to the surrounding soft and hard tissues, causing clinical complications [7–11]. Several breakthroughs in exodontia, such as periostomes, physics forceps, piezosurgery and various tooth extraction systems, have advanced safe tooth extraction. However, tools such as periostomes and piezosurgery implement the mechanical disruption of the PDL fibers while other appliances assisting in preserving bone socket dimensions by limiting the applied force to the vertical direction (e.g., the Benex<sup>®</sup> extraction system) [12–17]. Overall, these methods are based solely on the mechanical component, offering only a slight reduction in the amount of physical force required for tooth extraction.

Since enzymes can boost biochemical reaction rates [18], enzymatic degradation of the collagen fibers of the PDL prior to extraction per se could actually lead to a significant reduction in the physical force required for tooth delivery. Unlike mammalian collagenases that are part of matrix metalloproteinases (MMPs) [19–21] and usually cleave collagen at a single site, bacterial collagenases degrade collagen at multiple sites, turning collagen into short peptide fragments [22]. A variety of bacterial collagenases have been structurally and functionally characterized [23–30]. Among these, a truncated version of collagenase G of *Clostridium histolyticum* (ColG) was recombinantly expressed in *Escherichia coli* (*E. coli*), showing high expression yields [23, 31]. Indeed, several studies have analyzed and utilized enzymes or bacteria's ability to degrade collagen in the PDL, showing the feasibility of such biological-driven approaches [32–34]. Furthermore, native collagenase G extracted directly from *Clostridium histolyticum* is approved by the United States Food and Drug Administration (FDA) for treating Dupuytren's contracture and Peyronie diseases, characterized by abnormal collagen deposition [35–37], further confirming the feasibility of enzymatically-driven degradation of the PDL collagen fibers *in-vivo*.

Various biotechnological applications require highly stable recombinant proteins that do not negatively affect enzymatic activity rates. However, natural enzymes often evolve with a tradeoff between stability and activity [38], which may not always be suitable for the desired application. This necessitates enzyme optimization to achieve a specific profile. Indeed, therapeutic enzymes could greatly benefit from a higher thermal stability profile, resulting in longer shelf life, lower aggregation rates, reduced immunogenicity, and improved activity in tissues. Moreover, although this correlation does not apply to all enzymes, in many instances, a thermally stable structure is associated with better function and higher yields of recombinant expression [39–44].

Enzyme durability with a longer half-life can be achieved through alternative approaches such as

encapsulation or engineering of its structural features [45]. The latter can be accomplished using various computational approaches that have been developed to engineer protein variants with enhanced thermostability [46–51]. Although protein engineering is well established in a broad range of biotechnological and clinical applications [52, 53], its significance in dental medicine has not been demonstrated. Previous *in-silico* studies of collagenase focused on understanding the enzyme activity or analysis of the binding site, mainly for inhibiting the enzyme's catalytic activity [54–57]. However, enhanced thermostability of ColG and the effect on collagen degradation were not explored. Inspired by the successful application of collagenase in medicine [58, 59], we have previously shown that injection of ColG into the PDL significantly reduces the force required to extract roots of split first and second mandibular premolar teeth in an *ex-situ* jaw model of 6-month-old domestic swine [60]. Herein, we harnessed the PROSS computational protein engineering techniques and seek for mutations in the primary sequence of ColG to further improve its thermostability and collagenolytic activity. Implementing the PROSS algorithm was shown to improve protein stability and heterologous expression levels for a variety of challenging enzymes and proteins [61, 62]. The PROSS web server assembles new backbone combinations, starting from a set of homologous yet structurally diverse enzyme structures, to optimize the amino acid sequence while conserving key catalytic residues [63]. Our results show that the novel enzyme resulting from the PROSS computational engineering (ColG-variant) reduces the force required for tooth extraction compared to ColG.

## Results

### Computational design of ColG-variant

Having an established assay for *ex-situ* evaluation of forces required for tooth extraction [60], we embarked on the engineering of a collagenase with enhanced thermostability. From the various alternative solutions of PROSS, we selected the least permissive one, which involved replacing 17 amino acids along the protein backbone. These replacements accounted for ~2.5% of the total active site protein length. This design ensures that the enzyme maintains its overall structure and activity. Indeed, in a benchmark study that evaluated multiple PROSS designs, the least permissive design exhibited significant improvement in expressions levels and thermal stability profile.

In addition to the N-terminus collagenase catalytic domain (Tyr119-Gly790), the overall structure of ColG is composed of a single polycystic kidney disease-like (PKD-like) domain, and various collagen-binding domains (CBD) [23]. The crystal structure of the

N-terminus ColG reveals a saddle shape two-domain architecture. This latter shows full collagenolytic activity and is therefore selected as our template for further optimization. The catalytic domain comprises a highly conserved HEXXH Zn<sup>+2</sup> binding motif as well as an Ca<sup>+2</sup> binding site. Within this region, two conserved Gly, Gly493 and Gly494, the following edge strand—Leu495-Glu498 as well as Gln511-Phe515 are part of the collagenase substrate recognition site [29]. Figure 1A illustrates the position of the mutated amino acids on the ColG structure. As expected, most substitutions are

positioned on the protein's surface (purple residues in Fig. 1A), far from the active site of the enzyme. Moreover, the mutations do not interfere with the conserved Zn binding site residues or with the important collagen recognition site. This resulted in the replacement of surface-exposed hydrophobic groups into more hydrophilic residues. For example, F and G hydrophobic residues were mutated to Y/N/T hydrophilic residues in the F295Y, G670N and G672T positions. Figure 1B shows the sequence alignment of ColG and ColG-variant. In addition to hydrophobic to hydrophilic substitution, several

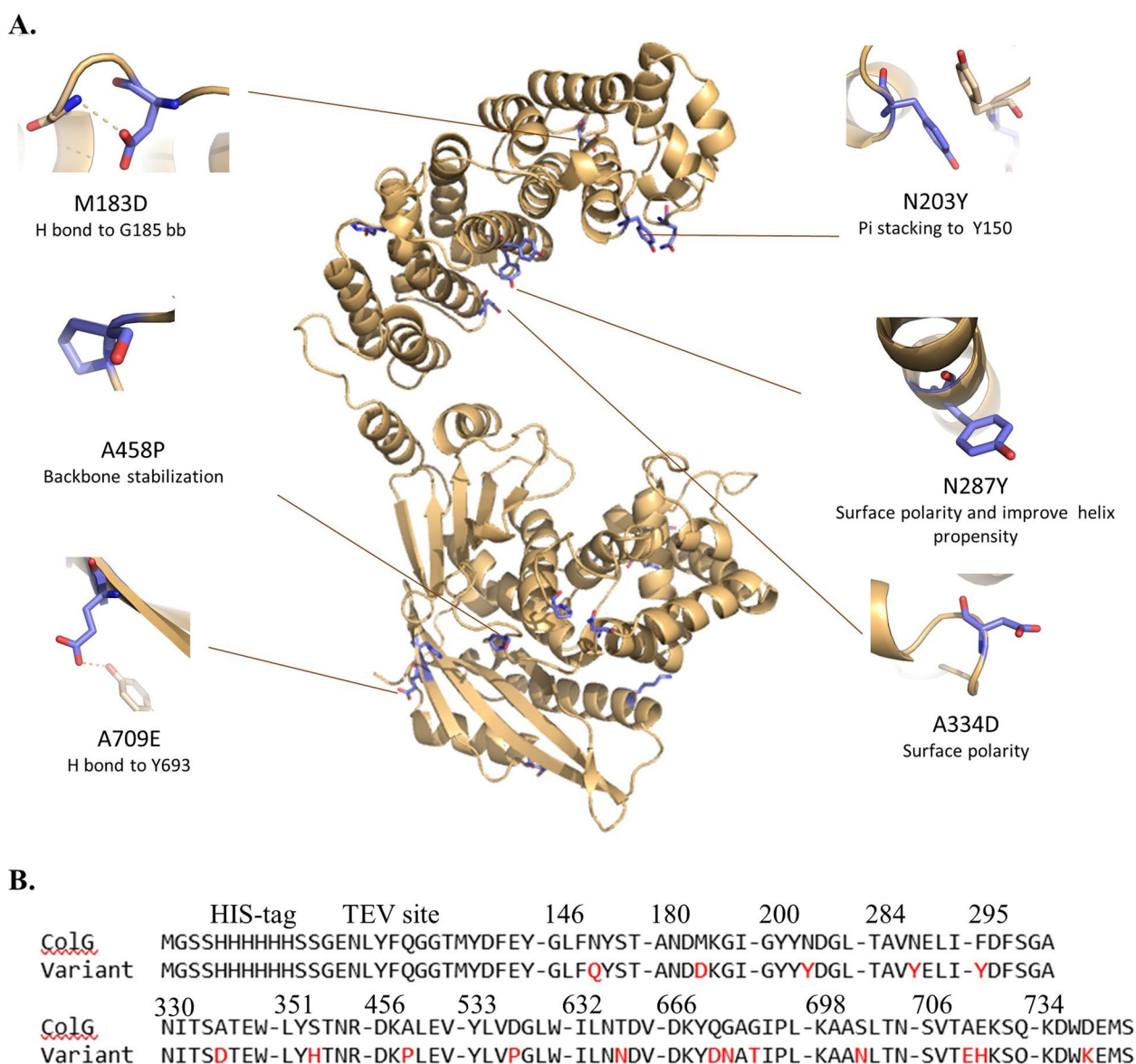


**Fig. 1** Illustration of ColG-variant. **A** The ColG structure is shown in brown, while mutations implemented in ColG-variant are depicted in purple (Selected mutations are shown). **B** Sequence alignment of ColG and ColG-variant in the specific regions, where mutations occurred (mutations in ColG-variant are denoted in red)

new interactions contribute to enhanced stability, such as hydrogen bonding. For instance, Met 183 to Asp sets an H bond with Gly 185, and Ala 709 to Glu forms an H bond with the side chain of Tyr 693. The G672T mutation also permits the formation of a Hydrogen bond of the side chain of the Thr with the back bone of Ile 673. Although contribution of a single hydrogen bonding to stability is not substantial, such a network is essential for determining protein folding and structure. An additional interaction that plays a role in protein stability is the coulomb interaction, driven by the aromatic side chains [64]. The stacking interaction is formed via the substitution of Asn 203 Tyr, which constructs a pi-pi interaction with Tyr 150. Moreover, the replacement of Asn 287 with Tyr leads to a stabilizing of its alpha helix [65]. Additional stabilizing mutations of residues that are located within a flexible loop are the substitution of Ala 458 and Asp 536 with Pro, leading to a more rigid conformation of the protein [66].

**Evaluation of ColG-variant’s thermostability**

To evaluate the thermostability of ColG-variant, we examined its ability to digest native collagen following the incubation of the enzyme at variable temperatures, ranging from 30 °C to 90 °C. For this purpose, we relied on the biochemical collagenolytic activity assay of 3,4-DHPAA [31, 67]. This experimental approach enables evaluation of the activity of collagenase on a native full-length collagen, rather than on collagen-derived peptides. Figure 2 shows the relative residual collagenolytic activity of ColG and ColG-variant as a function of the temperature. Before the activity assay, the enzymes were incubated at variable temperatures for one hour and then cooled down to 25°C. The

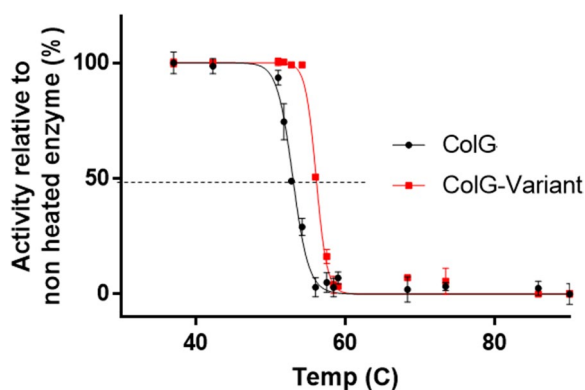


**Fig. 2** Tm Evaluation of ColG and ColG-variant. Enzymes were incubated at temperatures ranging from 30 °C to 90 °C for one hour and cooled down to 25 °C prior to the collagenolytic activity assay. Residual collagenolytic activity was plotted as a function of temperature for ColG (Black) and ColG-variant (Red). The data represent the mean of three replicates ± standard deviation

temperature at which the enzyme activity dropped to 50% relative to the activity of the non-heated enzyme is considered the melting temperature (Tm) of the enzyme. Thus, higher Tm suggests that the enzyme retained its activity at a higher temperature and is thus more thermostable. The Tm of ColG and the engineered ColG-variant were 52.9°C and 56.6°C, respectively. This suggests the enhanced thermostability of ColG-variant.

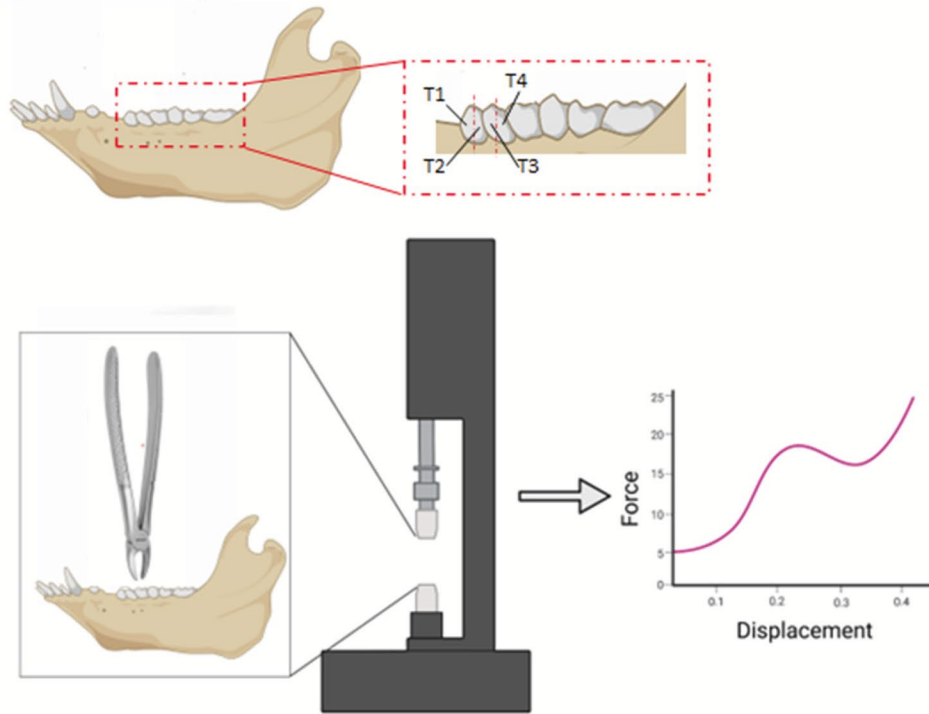
**Measurement of force required for root extraction**

To further evaluate the ability of the new enzyme to degrade collagen, we injected ColG-variant into the PDL of the split first and second mandibular premolar tooth roots (marked in Fig. 3A as T1 [mesial root of premolar 1], T2 [distal root of premolar 1], T3 [mesial root of premolar 2], and T4 [distal root of premolar 2]), in an *ex-situ* jaw model of 6-month-old domestic swine, as previously described [60]. ColG was injected into the corresponding roots on the contralateral side. Following incubation of 16 h, real-time recording of the pulling force vs. tooth displacement was performed using the tensile strength testing machine (Fig. 3A). Figure 3B shows the mean force (marked by a horizontal black line), as well as the values and dispersion of the root-specific maximal force applied to extract T1–4 in all jaws following treatment with ColG (blue) or ColG-variant (red). We found that the force required for extraction of each root was reduced with ColG-variant, by 12%, 13%, 8% and 6% for T1, T2, T3 and T4, respectively, with a total average reduction of 11%.

**Discussion**

Protein engineering is a robust approach commonly used for imparting specific activity profiles to proteins for a broad range of applications. However, the use of bio enzymes in the field of dental medicine was rarely explored. Herein, relying on the ability of collagenase G to degrade PDL collagen fibers *ex-situ*, we aimed to engineer an enzyme with enhanced thermostability. The latter characteristic is often associated with improved activity or used as the starting point for further optimization of the enzyme. The engineering of new protein variants is commonly achieved by directed evolution methods. In a typical directed evolution experiment, random or semi-rational mutagenesis is used to generate a library of the target gene from which optimized variants are isolated following several screening and selection rounds [68, 69]. However, wet-lab methods generally require extensive experiments and are not efficient, especially for discovering optimized catalytic activity of enzymes. On the other hand, computational approaches have been shown to be effective in designing new proteins *de-novo* or based on the structure of a native protein as the starting point [70–73]. Here, we have used the PROSS algorithm to improve ColG stability. The

**A. Experimental setup**



**B. Force required for each root extraction**

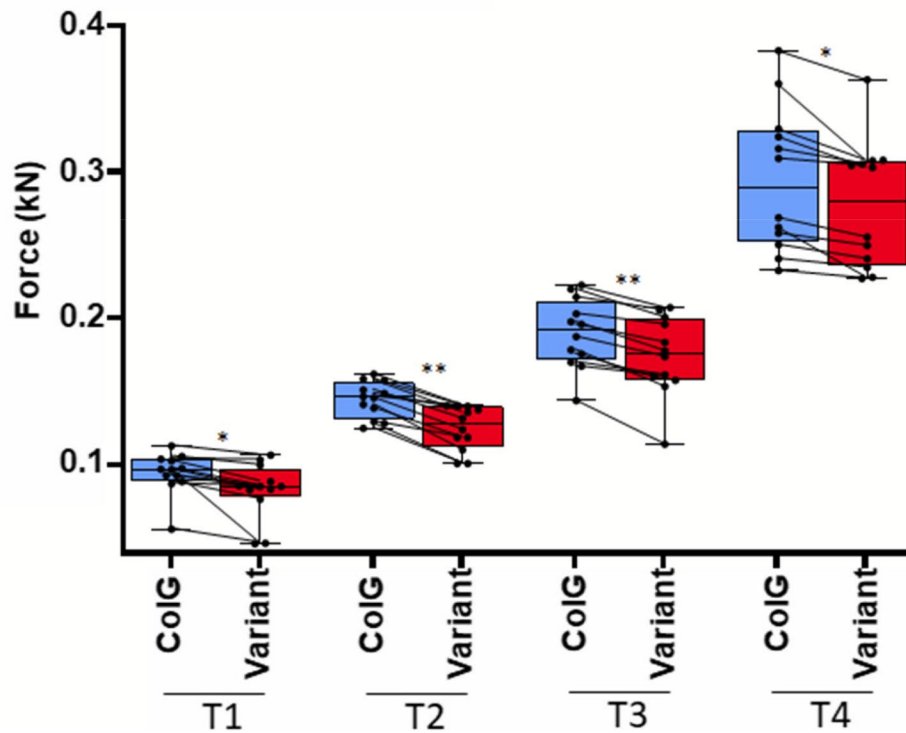


**Fig. 3** (See legend on next page.)

(See figure on previous page.)

**Fig. 3** Measurement of tooth extraction forces in porcine jaw. **A** The first and second porcine mandibular premolar teeth were split to form four roots labeled as T1, T2, T3 and T4. Following 16 h from the injection of ColG or its variant, the extraction was performed using the tensile strength testing machine along the longitudinal axes of each extracted root, and the force vs. displacement was recorded. **B** Mean and dispersion of extraction forces of ColG (blue) and ColG-variant (red). Each contralateral pair of roots is marked by black circles and connective lines, and the horizontal line marks the mean force for each root. Statistically significant values are indicated above each paired data, \*: $p < 0.01$ , \*\*: $p < 0.001$

algorithm has been successfully applied to various challenging enzymes and binding proteins, showing remarkable success in improving protein stability and expressibility, while maintaining wild-type activity levels [61]. Among the most dominant effects that govern protein folding and stability is the hydrophobic effect, whereby a-polar residues are buried within the stable protein structure, forming favorable Van Der Waals contact, while polar residues are presented at the protein surface [64]. Indeed, the point mutations in the ColG-variant (Fig. 1A) are located at the protein surface. Therefore, although every single mutation has a relatively low contribution to stability, the overall effect is not negligible.

The new ColG-variant was tested in two orthogonal assays. The first assay determined its thermostability by evaluating the ability of the enzyme to degrade collagen *in-vitro*, following incubation at varied temperatures. Enhanced thermostability is often correlated with improved characteristics that are important for an enzyme therapeutic application. In the context of enzymatically-driven exodontia, improved thermostability could mean accelerated degradation of the PDL collagen fibers due to better activity in the tissue and longer shelf life of the enzyme. We also noticed that albeit in a higher temperature, ColG-variant has a sharper activity decrease vs. temperature than its counterpart wild-type enzyme. This behavior is attributed to the enzyme's net of new interactions, however, with no expected implications on clinical aspects. The second assay tested the superiority of ColG-variant in reducing the forces required for tooth extraction *ex-situ*, compared to ColG [60]. This may have a significant impact on the morbidity, implying fewer intra- and post-operative complications and reduced damage to soft and hard tissues surrounding the tooth being extracted. Furthermore, atraumatic or minimally invasive exodontia can facilitate the subsequent implant placement and restoration, thus shortening the overall time from procedure to final rehabilitation. Additional factors should be examined further, such as the reduction of the time period required from the moment of injection of the enzyme to extraction per se and the evaluation of minimal enzyme concentration that could lead to sufficient force reduction. Moreover, future research should evaluate the potency of ColG-variant in an *in-vivo* environment, additionally characterized

by blood circulation and efficient regulatory immune system, which could affect the enzyme's activity as well as its half-life in the tissue. Ultimately, considering the existing clinical applications of collagenase G, purified directly from *Clostridium histolyticum*, in orthopedics (i.e., Dupuytren's contracture) [74, 75] and urology (i.e., Peyronie disease) [76], dental application of ColG-variant, characterized by enhanced thermostability, should be feasible.

## Conclusions

The research shows for the first time the application of engineered proteins in dental medicine. The engineering of an improved thermal-stable collagenase further reduces the force required for tooth extraction. It is concluded that the application of engineered biomolecules to impart a desired activity profile can advance non-invasive dental medicine.

## Methods

### Computational enzyme design

The initial structure of ColG is based on collagenase G from *Clostridium histolyticum* (PDB 4ARE) [25]. The catalytic domain of ColG comprises Tyr 119—Ala 790 [23], while the catalytic pocket itself ranges from Asp 398 to Gly 790 [29]. Zn<sup>2+</sup> and Ca<sup>2+</sup> ions are located at the catalytic domain and are essential for the enzymatic catalytic reaction [25]. To generate a more thermally stable variant, we initially relied on PDB structure 4ARE, maintaining its catalytic domain and the Zn<sup>2+</sup> ion. However, the structure lacks the active Ca<sup>2+</sup> ion. Therefore, as a preliminary preparation step, we replaced a water molecule within the enzyme cavity, with a Ca<sup>2+</sup> ion. The latter was based on the well-resolved structure of collagenase H (ColH), PDB 4ARE. The modified structure was inserted into the PROSS web server (<https://pross.weizmann.ac.il/step/pross-terms/>). The PROSS web server assembles new backbone combinations, starting from a set of homologous yet structurally diverse enzyme structures, to optimize the amino acid sequence while conserving key catalytic residues [63]. PROSS uses phylogenetic analysis in combination with Rosetta atomistic design calculation in order to generate a set of mutations that are assumed to improve protein stability. PROSS conserves the essential amino acid sequence and side-chain

conformations at the active site, yet, applies stabilizing mutations that are not rare among other homologs [61]. The two ions and their surrounding residues, especially the highly conserved residues, important for ion binding,—Glu 498, His 523, Glu 524 and His 527, were held constant throughout the calculations.

### Protein expression and purification

Hans Brandstetter [23, 25] generously provided the gene of ColG containing residues Tyr119-Lys1118 with an N-terminus His-tag followed by a TEV cleavage site. The gene of the new enzyme variant originating from PROSS was synthesized and cloned into the same pET15b vector. The plasmid was transformed into competent *E.coli* BL21(DE3) on an ampicillin agar plate. Colonies were transferred to Luria Growth (LB) medium supplemented with ampicillin (100ug/ul), and at  $OD_{600}=0.8$ , protein expression was induced with the addition of 1 mM IPTG. For protein purification, cells were centrifuged, resuspended in a lysis buffer (50 mM NaPi, 300 mM NaCl, 10 mM Imidazole, pH=8) and sonicated so as to disrupt them. The soluble protein fraction was isolated by centrifugation at 10,000 g, and the supernatant was applied to a 5 ml  $Ni^{2+}$  HisTrap FF column (Cytiva, USA). Following extensive washing with buffer-1 (50 mM NaPi, 300 mM NaCl, 40 mM imidazole, pH=8), buffer-2 (50 mM NaPi, 1 M NaCl, 10 mM imidazole, pH=8) and buffer-3 (50 mM NaPi, 300 mM NaCl, 20% Glycerol, pH=8), the protein was eluted with buffer-1 containing 300 mM Imidazole. The elution fraction was concentrated using an Amicon Ultra-15 (Merck, USA) concentration tube (30,000-MWCO), and the buffer was changed to PBS by dialysis.

### Thermal stability assay

Thermal stability was evaluated by incubating 80  $\mu$ l of the purified enzymes in a concentration of 200  $\mu$ g/ml in 50 mM TRIS 5 Mm  $CaCl_2$  pH=7.5 for 30 min in a PCR thermal cycler (C1000 touch, Bio-Rad, Germany). Incubation was carried out in variable temperatures, ranging from 37°C to 90°C. Residual activity was then measured and compared with the activity of the unheated enzyme. The biochemical assay was performed based on the previously described protocol [31, 67]. The purified enzyme was incubated with collagen-I, and aliquots were mixed with 50 mM Tris buffer (pH=7.5), 5 mM  $CaCl_2$  at a total volume of 200  $\mu$ l in a 96 well plate at 37 °C. Aliquots of 50  $\mu$ l were then mixed with 50  $\mu$ l of 0.75 mM 3,4-DHPAA, 50ul of 125 mM sodium borate (pH=8.0) and 50  $\mu$ l of 1.25 mM  $NaIO_4$ ; and incubated for 30 min at 37 °C. The fluorescence intensity of the reaction mixture was measured by a spectrofluorometer (BioTek,

Winoosky, VT, USA). The excitation and emission maxima were 375 nm and 465 nm, respectively.

### Jaw preparation and injection of collagenase into the PDL

The whole mandibles of a 6-month-old (90–100 kg) domestic swine close to slaughter were obtained from a local abattoir (Marsel Brothers Company, Haifa, Israel). A specially designed jaw stabilization device was employed, as previously described [60] and illustrated in Fig. 3A. Either ColG or its variant was injected into the PDL of contralateral roots of a mandibular porcine split first and second premolar teeth with the Wand Single Tooth Anesthesia System (Milestone Scientific, New Jersey, USA), as previously described [60]. Briefly, the outer soft tissues adjacent to the teeth were removed. Then, the first and second mandibular premolar teeth (PM1 and PM2, respectively), which contain two divergent roots, were split into four different roots T1, T2, T3 and T4 (Fig. 3A) [60]. Standard cartridges containing the local anesthetic solution for dental injection were emptied of their content and filled with either ColG or ColG-variant at a concentration of 4ug/ul. The injection was performed using a needle of 30G 2.54 cm that was inserted into the PDL space and advanced apically until stopped by the resistance of the alveolar bone proper. The injection was repeated at four sites around each root, on the buccal, lingual, mesial, and distal aspects. A total of 0.3 ml of 4  $\mu$ g/ $\mu$ l was injected. Concentration was selected based on previous studies and clinical practice for injection of wild-type collagenase G for Dupuytren's disease [60, 77].

### Measurement of force required for root extraction

The extraction force was applied by a loading machine (Instron Series 6800; Instron Corp., Canton, MA, USA) using a load cell of 2 kilonewtons and a crosshead speed of 10 mm/minute, until the root was completely removed from the alveolar socket. The force was recorded at a rate of 10 Hz. Assessment of the tensile force and displacement during the root extraction process was achieved via the designated software (Instron Series IX; Instron Corp.).

### Statistical analysis

Statistical comparisons between the force of the different extracted roots were performed by a paired t-test with two-tail distribution with unequal variance. For statistical analysis, significance was set as  $*=0.01 \leq p < 0.05$ ;  $**=p < 0.01$ .

### Graphics

Figure 3 was created with BioRender.

**Abbreviations**

PDL	Periodontal ligament
ColG	Collagenase G
MMPs	Matrix Metalloproteinase
WT	Wild type
FDA	Food and Drug Administration
PDB	Protein Data Bank
LB	Luria Broth

**Supplementary Information**

The online version contains supplementary material available at <https://doi.org/10.1186/s13036-023-00366-4>.

**Additional file 1.**

**Authors' contributions**

T.A conducted all computational analysis and design. R.T, A.C, O.C and A.A conducted the experiments and analyzed the data. S.M, S.L, D.Z.B contributed to the conception of the study. D.Z.B and T.A assisted with data and statistical analysis. M.G and E.W conceived the research idea, and supervised the research. T.A, M.G and E.W wrote the final version of the manuscript. All the authors approved the final version of the manuscript.

**Funding**

The research was supported from funding of the Faculty of Medicine of Tel Aviv University to the lab of M.G.

**Availability of data and materials**

All data generated or analyzed during this study are included in this published article and its [Supplementary information](#) files.

**Declarations**

**Ethics approval and consent to participate**

Not applicable.

**Consent for publication**

Not applicable.

**Competing interests**

T.A, R.T, E.W and M.G. submitted patent application PCT/IL2022/051304. E.W is the co-founder of PROTEOLASE Ltd. and the inventor of US patent no. 10016492.

Received: 7 May 2023 Accepted: 5 July 2023

Published online: 17 July 2023

**References**

1. Sambrook PJ, Goss AN. Contemporary exodontia. *Aust Dent J*. 2018;63(Suppl 1):S11–8.
2. McKenzie WS. Principles of exodontia. *Oral Maxillofac Surg Clin North Am*. 2020;32:511–7.
3. Kaku M, Yamauchi M. Mechano-regulation of collagen biosynthesis in periodontal ligament. *J Prosthodont Res*. 2014;58:193–207.
4. Naveh GRS, Brumfeld V, Shahar R, Weiner S. Tooth periodontal ligament: Direct 3D microCT visualization of the collagen network and how the network changes when the tooth is loaded. *J Struct Biol*. 2013;181:108–15.
5. Jain A. Principles and Techniques of Exodontia. In: Bonanathaya K, Panneerselvam E, Manuel S, Kumar VV, Rai A, editors. *Oral and Maxillofacial Surgery for the Clinician*. Singapore: Springer Nature Singapore; 2021. p. 259–97.
6. Niemiec BA. Periodontal flap surgery. *Veterinary Periodontology*. West Sussex: Wiley; 2013. p. 206–48.

7. Vettori E, Constantinides F, Nicolin V, Rizzo R, Perinetti G, Maglione M, et al. Factors influencing the onset of intra- and post-operative complications following tooth exodontia: retrospective survey on 1701 patients. *Antibiotics (Basel)*. 2019;8:264. <https://doi.org/10.3390/antibiotics8040264>.
8. Lorè B, Gargari M, Ventucci E, Cagioli A, Nicolai G, Calabrese L. A complication following tooth extraction: chronic suppurative osteomyelitis. *Oral Implantol*. 2013;6:43–7.
9. Tong AC, Leung AC, Cheng JC, Sham J. Incidence of complicated healing and osteoradionecrosis following tooth extraction in patients receiving radiotherapy for treatment of nasopharyngeal carcinoma. *Aust Dent J*. 1999;44:187–94.
10. Cohen N, Cohen-Lévy J. Healing processes following tooth extraction in orthodontic cases. *J Dentofac Anomal Orthodontics*. 2014;17:304 Éditions SID, Groupe EDP Sciences.
11. Dudek D, Marchionni S, Gabriele M, Iurlaro A, Helewski K, Toti P, et al. Bleeding rate after tooth extraction in patients under oral anticoagulant therapy. *J Craniofac Surg*. 2016;27:1228–33.
12. Blus C, Szmukler-Moncler S. Atraumatic tooth extraction and immediate implant placement with Piezosurgery: evaluation of 40 sites after at least 1 year of loading. *Int J Periodontics Restorative Dent*. 2010;30:355–63.
13. Sharma SD, Vidya B, Alexander M, Deshmukh S. Periostome as an aid to atraumatic extraction: a comparative double blind randomized controlled trial. *J Maxillofac Oral Surg*. 2015;14:611–5.
14. Garg AK. Using the Piezosurgery device: basics and possibilities. *Dent Implantol Update*. 2007;18:1–4.
15. Schlee M, Steigmann M, Bratu E, Garg AK. Piezosurgery: basics and possibilities. *Implant Dent*. 2006;15:334–40.
16. Hong B, Bulsara Y, Gorecki P, Dietrich T. Minimally invasive vertical versus conventional tooth extraction: an interrupted time series study. *J Am Dent Assoc*. 2018;149:688–95.
17. Muska E, Walter C, Knight A, Taneja P, Bulsara Y, Hahn M, et al. Atraumatic vertical tooth extraction: a proof of principle clinical study of a novel system. *Oral Surg Oral Med Oral Pathol Oral Radiol*. 2013;116:e303–10.
18. Warshel A, Sharma PK, Kato M, Xiang Y, Liu H, Olsson MHM. Electrostatic basis for enzyme catalysis. *Chem Rev*. 2006;106:3210–35.
19. Laronha H, Caldeira J. Structure and function of human matrix metalloproteinases. *Cells*. 2020;9:1076. <https://doi.org/10.3390/cells9051076>.
20. Amar S, Smith L, Fields GB. Matrix metalloproteinase collagenolysis in health and disease. *Biochim Biophys Acta Mol Cell Res*. 2017;1864:1940–51.
21. Quintero-Fabián S, Arreola R, Becerril-Villanueva E, Torres-Romero JC, Arana-Argáez V, Lara-Riegos J, et al. Role of matrix metalloproteinases in angiogenesis and cancer. *Front Oncol*. 2019;9:1370.
22. Duarte AS, Correia A, Esteves AC. Bacterial collagenases - a review. *Crit Rev Microbiol*. 2016;42:106–26.
23. Eckhard U, Nüss D, Ducka P, Schönauer E, Brandstetter H. Crystallization and preliminary X-ray characterization of the catalytic domain of collagenase G from *Clostridium histolyticum*. *Acta Crystallogr Sect F Struct Biol Cryst Commun*. 2008;64:419–21.
24. Ohbayashi N, Matsumoto T, Shima H, Goto M, Watanabe K, Yamano A, et al. Solution structure of clostridial collagenase H and its calcium-dependent global conformation change. *Biophys J*. 2013;104:1538–45.
25. Eckhard U, Schönauer E, Brandstetter H. Structural basis for activity regulation and substrate preference of clostridial collagenases G, H, and T. *J Biol Chem*. 2013;288:20184–94.
26. Abfalter CM, Schönauer E, Ponnuraj K, Huemer M, Gadermaier G, Regl C, et al. Cloning, Purification and Characterization of the Collagenase ColA Expressed by *Bacillus cereus* ATCC 14579. *PLoS ONE*. 2016;11:e0162433.
27. Chen S, Ma M, Fu X. Analyzing structural and functional characteristics of collagenase from *Bacillus cereus* MH19 via in silico approaches. *Curr Proteomics*. 2020;17:200–12 Bentham Science Publishers Ltd.
28. Ikeuchi T, Yasumoto M, Takita T, Tanaka K, Kusubata M, Hayashida O, et al. Crystal structure of *Grimontia hollisiae* collagenase provides insights into its novel substrate specificity toward collagen. *J Biol Chem*. 2022;298:102109.
29. Eckhard U, Schönauer E, Nüss D, Brandstetter H. Structure of collagenase G reveals a chew-and-digest mechanism of bacterial collagenolysis. *Nat Struct Mol Biol*. 2011;18:1109–14.
30. Bauer R, Janowska K, Taylor K, Jordan B, Gann S, Janowski T, et al. Structures of three polycystic kidney disease-like domains from *Clostridium*

- histolyticum collagenases ColG and ColH. *Acta Crystallogr D Biol Crystallogr*. 2015;71:565–77.
31. Tohar R, Ansbacher T, Sher I, Afriat-Jurnou L, Weinberg E, Gal M. Screening collagenase activity in bacterial lysate for directed enzyme applications. *Int J Mol Sci*. 2021;22:8552. <https://doi.org/10.3390/ijms22168552>.
  32. Zinger A, Adir O, Alper M, Simon A, Poley M, Tzror C, et al. Proteolytic nanoparticles replace a surgical blade by controllably remodeling the oral connective tissue. *ACS Nano*. 2018;12:1482–90.
  33. Ujiie Y, Shimada A, Komatsu K, Gomi K, Oida S, Arai T, et al. Degradation of noncollagenous components by neutrophil elastase reduces the mechanical strength of rat periodontal ligament. *J Periodontol Res*. 2008;43:22–31.
  34. Sela MN, Kohavi D, Krausz E, Steinberg D, Rosen G. Enzymatic degradation of collagen-guided tissue regeneration membranes by periodontal bacteria. *Clin Oral Implants Res*. 2003;14:263–8.
  35. Smeraglia F, Del Buono A, Maffulli N. Collagenase clostridium histolyticum in Dupuytren's contracture: a systematic review. *Br Med Bull*. 2016;118:149–58.
  36. Gabrielson AT, Spitz JT, Hellstrom WJG. Collagenase clostridium histolyticum in the treatment of urologic disease: current and future impact. *Sex Med Rev*. 2018;6:143–56.
  37. Warwick D, Arandes-Renú JM, Pajardi G, Witthaut J, Hurst LC. Collagenase Clostridium histolyticum: emerging practice patterns and treatment advances. *J Plast Surg Hand Surg*. 2016;50:251–61.
  38. Littlechild JA. Enzymes from extreme environments and their industrial applications. *Front Bioeng Biotechnol*. 2015;3:161.
  39. Lippow SM, Tidor B. Progress in computational protein design. *Curr Opin Biotechnol*. 2007;18:305–11.
  40. Shire SJ, Shahrokh Z, Liu J. Challenges in the development of high protein concentration formulations. *J Pharm Sci*. 2004;93:1390–402.
  41. Hermeling S, Crommelin DJA, Schellekens H, Jiskoot W. Structure-immunogenicity relationships of therapeutic proteins. *Pharm Res*. 2004;21:897–903.
  42. Braun A, Kwee L, Labow MA, Alsenz J. Protein aggregates seem to play a key role among the parameters influencing the antigenicity of interferon alpha (IFN-alpha) in normal and transgenic mice. *Pharm Res*. 1997;14:1472–8.
  43. Shoichet BK, Baase WA, Kuroki R, Matthews BW. A relationship between protein stability and protein function. *Proc Natl Acad Sci U S A*. 1995;92:452–6.
  44. Carlin DA, Hapig-Ward S, Chan BW, Damrau N, Riley M, Caster RW, et al. Thermal stability and kinetic constants for 129 variants of a family 1 glycoside hydrolase reveal that enzyme activity and stability can be separately designed. *PLoS ONE*. 2017;12:e0176255.
  45. Shimanovich U, Ruggeri FS, De Genst E, Adamcik J, Barros TP, Porter D, et al. Silk micrococoon for protein stabilisation and molecular encapsulation. *Nat Commun*. 2017;8:15902.
  46. Pires DEV, Ascher DB, Blundell TL. DUET: a server for predicting effects of mutations on protein stability using an integrated computational approach. *Nucleic Acids Res*. 2014;42:W314–9 Oxford Academic.
  47. Capriotti E, Fariselli P, Casadio R. I-Mutant2.0: predicting stability changes upon mutation from the protein sequence or structure. *Nucleic Acids Res*. 2005;33:W306–10.
  48. Laimer J, Hiebl-Flach J, Lengauer D, Lackner P. MAESTROweb: a web server for structure-based protein stability prediction. *Bioinformatics*. 2016;32:1414–6.
  49. Wijma HJ, Floor RJ, Jekel PA, Baker D, Marrink SJ, Janssen DB. Computationally designed libraries for rapid enzyme stabilization. *Protein Eng Des Sel*. 2014;27:49–58.
  50. Schymkowitz J, Borg J, Stricher F, Nys R, Rousseau F, Serrano L. The FoldX web server: an online force field. *Nucleic Acids Res*. 2005;33:W382–8.
  51. Bednar D, Beerens K, Sebestova E, Bendl J, Khare S, Chaloupkova R, et al. FireProt: energy- and evolution-based computational design of thermostable multiple-point mutants. *PLoS Comput Biol*. 2015;11:e1004556.
  52. Meghwanshi GK, Kaur N, Verma S, Dabi NK, Vashishtha A, Charan PD, et al. Enzymes for pharmaceutical and therapeutic applications. *Biotechnol Appl Biochem*. 2020;67:586–601.
  53. Victorino da Silva Amatto I, Gonsales da Rosa-Garzon N, Antônio de Oliveira Simões F, Santiago F, Pereira da Silva Leite N, Martins J, et al. Enzyme engineering and its industrial applications. *Biotechnol Appl Biochem*. 2022;69:389–409.
  54. Eckhard U, Huesgen PF, Brandstetter H, Overall CM. Proteomic protease specificity profiling of clostridial collagenases reveals their intrinsic nature as dedicated degraders of collagen. *J Proteomics*. 2014;100:102–14.
  55. Hartmann A, Gostner J, Fuchs JE, Chaita E, Aliagiannis N, Skaltsounis L, et al. Inhibition of collagenase by mycosporine-like amino acids from marine sources. *Planta Med*. 2015;81:813–20.
  56. Eun Lee K, Bharadwaj S, Yadava U, Gu KS. Evaluation of caffeine as inhibitor against collagenase, elastase and tyrosinase using in silico and in vitro approach. *J Enzyme Inhib Med Chem*. 2019;34:927–36.
  57. Kumar V, Srikaku N, Aathmanathan VS, Satheeshkumar PK, Madathiparambil MG, Krishnan M, et al. Molecular modeling and virtual screening of molecular inhibitors for leptospiral collagenase. *Research Square*. Research Square; 2021. Available from: <https://www.researchsquare.com/article/rs-259091/v1>.
  58. Kawada K, Komatsu K. In vitro effects of collagenase on biomechanical properties and morphological features of the rat molar periodontal ligament. *Jpn J Oral Biol*. 2000;193–205. <https://doi.org/10.2330/joralbiosci1965.42.193>.
  59. Komatsu K, Shibata T, Shimada A. Analysis of contribution of collagen fibre component in viscoelastic behaviour of periodontal ligament using enzyme probe. *J Biomech*. 2007;40:2700–6.
  60. Tohar R, Alali H, Ansbacher T, Brosh T, Sher I, Gafni Y, et al. Collagenase administration into periodontal ligament reduces the forces required for tooth extraction in an ex situ porcine jaw model. *J Funct Biomater*. 2022;13:76. <https://doi.org/10.3390/jfb13020076>.
  61. Peleg Y, Vincetelli R, Collins BM, Chen K-E, Livingstone EK, Weerantunga S, et al. Community-wide experimental evaluation of the PROSS stability-design method. *J Mol Biol*. 2021;433:166964.
  62. Goldenzweig A, Goldsmith M, Hill SE, Gertman O, Laurino P, Ashani Y, et al. Automated structure- and sequence-based design of proteins for high bacterial expression and stability. *Mol Cell*. 2016;63:337–46.
  63. Lapidoth G, Khersonsky O, Lipsh R, Dym O, Albeck S, Rogotner S, et al. Highly active enzymes by automated combinatorial backbone assembly and sequence design. *Nat Commun*. 2018;9:2780.
  64. Goldenzweig A, Fleishman SJ. Principles of protein stability and their application in computational design. *Annu Rev Biochem*. 2018;87:105–29.
  65. Pace CN, Scholtz JM. A helix propensity scale based on experimental studies of peptides and proteins. *Biophys J*. 1998;75:422–7.
  66. Matthews BW, Nicholson H, Becktel WJ. Enhanced protein thermostability from site-directed mutations that decrease the entropy of unfolding. *Proc Natl Acad Sci U S A*. 1987;84:6663–7.
  67. Yasmin H, Kabashima T, Rahman MS, Shibata T, Kai M. Amplified and selective assay of collagens by enzymatic and fluorescent reactions. *Sci Rep*. 2014;4:4950.
  68. Seitz T, Thoma R, Schoch GA, Stihle M, Benz J, D'Arcy B, et al. Enhancing the stability and solubility of the glucocorticoid receptor ligand-binding domain by high-throughput library screening. *J Mol Biol*. 2010;403:562–77.
  69. Packer MS, Liu DR. Methods for the directed evolution of proteins. *Nat Rev Genet*. 2015;16:379–94.
  70. Pirogova E, Istivan T. Toward development of novel peptide-based cancer therapeutics: computational design and experimental evaluation. In: Wang X, editor. *Bioinformatics of Human Proteomics*. Dordrecht: Springer, Netherlands; 2013. p. 103–26.
  71. Istivan TS, Pirogova E, Gan E, Almansour NM, Coloe PJ, Cosic I. Biological effects of a de novo designed myxoma virus peptide analogue: evaluation of cytotoxicity on tumor cells. *PLoS ONE*. 2011;6:e24809.
  72. Correia BE, Ban YEA, Holmes MA, Xu H, Ellingson K, Kraft Z, et al. Computational design of epitope-scaffolds allows induction of antibodies specific for a poorly immunogenic HIV vaccine epitope. *Structure*. 2010;18:1116–26.
  73. Khoury GA, Smadbeck J, Kieslich CA, Floudas CA. Protein folding and de novo protein design for biotechnological applications. *Trends Biotechnol*. 2014;32:99–109.

74. Shih B, Bayat A. Scientific understanding and clinical management of Dupuytren disease. *Nat Rev Rheumatol*. 2010;6:715–26.
75. Shubinets V, Lin IC, Chang B. Carpal tunnel syndrome after Xiaflex injection for Dupuytren disease. *Plast Reconstr Surg*. 2017;139:1031e–2e.
76. Gelbard M, Goldstein I, Hellstrom WJG, McMahon CG, Smith T, Tursi J, et al. Clinical efficacy, safety and tolerability of collagenase clostridium histolyticum for the treatment of peyronie disease in 2 large double-blind, randomized, placebo controlled phase 3 studies. *J Urol Ovid Technologies (Wolters Kluwer Health)*. 2013;190:199–207.
77. Costas B, Coleman S, Kaufman G, James R, Cohen B, Gaston RG. Efficacy and safety of collagenase clostridium histolyticum for Dupuytren disease nodules: a randomized controlled trial. *BMC Musculoskelet Disord*. 2017;18:374.

### **Publisher's Note**

Springer Nature remains neutral with regard to jurisdictional claims in published maps and institutional affiliations.

**Ready to submit your research? Choose BMC and benefit from:**

- fast, convenient online submission
- thorough peer review by experienced researchers in your field
- rapid publication on acceptance
- support for research data, including large and complex data types
- gold Open Access which fosters wider collaboration and increased citations
- maximum visibility for your research: over 100M website views per year

**At BMC, research is always in progress.**

Learn more [biomedcentral.com/submissions](https://biomedcentral.com/submissions)

